ELSEVIER

Biochimica et Biophysica Acta 1326 (1997) 103–114

BIOCHIMICA ET BIOPHYSICA ACTA
BBA

X-ray diffraction study of bilayer to non-bilayer phase transitions in aqueous dispersions of di-polyenoic phosphatidylethanolamines

W. Patrick Williams [a,*], A.P.R. Brain [a], Beth A. Cunningham [b], D.H. Wolfe [c]

[a] *Life Sciences Division, King's College London, Campden Hill, London W8 7AH, UK*
[b] *Department of Physics, Bucknell University, Lewisburg, PA 17837, USA*
[c] *Department of Astronomy and Physics, Lycoming College, Williamsport, PA 17701, USA*

Received 13 November 1996; accepted 23 January 1997

Abstract

The low temperature phase properties of aqueous dispersions of di-18:2 and di-18:3 phosphatidylethanolamine are strongly influenced by the presence of ice. In the presence of cryoprotectants to inhibit ice formation, these lipids persist in the H_{II} phase down to at least $-50°C$. Ice formation, however, leads to a drastic reduction in the amount of available free water and a rapid reduction in the diameter of the inverted cylindrical micelles of the H_{II} phase. The resulting increase in surface curvature of the micelles induces an imbalance in the forces acting in the lipid surface and the hydrophobic core which is relieved by formation of the L_α phase. On reheating the lipid samples undergo an abrupt $L_\alpha \rightarrow H_{II}$ phase transition at about $-20°C$. The radius of the water core of the inverted micelles at their point of formation is estimated to be 0.9 nm. This increases with temperature as more unfrozen water becomes available until the normal equilibrium radius of about 2.3 nm is reached at 0°C when the bulk water in the sample finally melts. A small proportion of the H_{II} phase lipid enters an as yet unidentified cubic phase on freezing. The spacings of the (10) planes of the H_{II} phase, the (111) planes of the cubic phase and the d-spacing of the L_α phase were found to be almost identical at the phase transition temperature. The cubic phase appears to disappear at low temperature but to reform on heating. Freeze-fracture studies revealed no unequivocal evidence for cubic phase lipid but the presence of residual non-bilayer lipid structures was observed even at temperatures as low as $-80°C$. The presence of intersecting stacks of lamellar sheets in the replicas strongly suggest the existence of an epitaxial relationship between the L_α and H_{II} phases in these systems.

Keywords: Phospholipid; Phosphatidylethanolamine; Polyenoic lipid; X-ray diffraction; Lipid phase behaviour

1. Introduction

An extensive literature exists regarding the phase behaviour of membrane lipids. The bulk of this literature relates to fully saturated lipids which are comparatively rare in natural membranes; it has, nevertheless, provided an invaluable framework for understanding many aspects of membrane behaviour. It has become increasingly clear, however, that the proper-

Abbreviations: PC, phosphatidylcholine; PE, phosphatidylethanolamine; MGDG, monogalactosyldiacylglycerol; L_α, liquid-crystal lamellar phase; L_β, gel lamellar phase; H_{II}, inverted hexagonal phase; L_c crystal (sub-gel) lamellar phase; T_m, gel to liquid crystal phase transition temperature; dioleoyl- (di-18:1) dilinoleoyl- (di-18:2), and dilinolenoyl- (di-18:3) PC and PE

* Corresponding author. Fax: +44 171 3334500.

PII S0005-2736(97)00017-5

ties of many of the more unsaturated species of lipid that represent major components of animal and plant cell membranes cannot easily be predicted by extrapolation of data collected for their more saturated counterparts. This has led to increasing interest in the physical properties of polyunsaturated membrane lipids.

Considerable information is available regarding the effects of the presence of multiple *cis*-double bonds on the gel to lamellar liquid-crystal (L_β-L_α) transitions of membrane lipids. The phase properties of series of mixed-acid 1,2-diacyl-3-phosphatidylcholine (PC) derivatives containing 16:0, 18:0 or 20:0 residues in the *sn*-1 position and polyenoic residues in the *sn*-2 position have been extensively studied using calorimetry [1–3], ^{2}H NMR [4,5] and Raman spectroscopy [6].

Introduction of a single *cis*-double bond into the chain in the *sn*-2 position of a fully saturated PC derivative can, depending on the position of the double bond [7,8], lower the temperature of the L_β-L_α phase transition, T_m, by up to 50°C. Smaller decreases are seen on introduction of a second *cis*-double bond reflecting the already perturbed state of the chain and the introduction of further double bonds may even lead to small increases in T_m [1,3].

The molar enthalpy of the transitions shows a similar pattern of reductions. In most cases, however, the transitions remain reasonably sharp indicating a high degree of co-operativity [3,5]. No systematic studies of this type have been carried out for other lipid classes but the available literature on individual lipid species suggest that they follow similar patterns of behaviour.

The introduction of a second polyenoic chain has an even more marked effect on the properties of the L_β-L_α transition of membrane lipids. Keough and Kariel [9] showed that PC derivatives containing two identical polyunsaturated chains are characterised by very broad, low enthalpy $L_\beta \rightarrow L_\alpha$ transitions starting at temperatures around -70°C and spanning ranges of approx. 40°C. We have confirmed their observations using X-ray diffraction measurements and extended them to include di-polyenoic phosphatidylethanolamine (PE) [10,11] and monogalactosyldiacylglycerol (MGDG) [12] derivatives. The breadth of the L_β-L_α transitions in the di-polyenoic PC and PE derivatives was shown to reflect the fact that they are second order transitions progressing through a continuum of stable intermediate states. This behaviour appears to be associated with the existence in these lipids of relatively disordered low-temperature gel L_β states in which the extended acyl chains of the lipids are centred on a regular hexagonal lattice but show little coherent packing [11].

Relatively little work has been carried out on the effect of unsaturation on bilayer to non-bilayer (L_α-H_{II}) transitions of lipids such as PE. This transition occurs at 101°C in di-18:0 PE [13] and is lowered to about 8°C in di-18:1 PE [14,15]. In a preliminary study, we showed that di-18:2 PE converts from the H_{II} to the L_α phase on the freezing of supercooled aqueous dispersions and converts back to the H_{II} when the samples start to melt [16]. Comparatively little is known, however, about the effects of multiple *cis* double bonds and ice formation on L_α-H_{II} transitions.

In this paper, we investigate the L_α-H_{II} transition occurring in aqueous dispersions of the di-polyenoic PE derivatives di-18:2 and di-18:3 PE. The $H_{II} \rightarrow L_\alpha$ transition observed on cooling, is shown to be driven by the formation of ice and the subsequent dehydration of the sample. The $L_\alpha \rightarrow H_{II}$ transition occurring on reheating is a classical first order transition but its extent is controlled by the availability of unfrozen water to rehydrate the sample. We demonstrate that the $H_{II} \rightarrow L_\alpha$ transition is accompanied by the concomitant formation of a cubic phase and present evidence suggesting an epitaxial relationship between the L_α, H_{II} and cubic phases.

2. Materials and methods

Synthetic L-di-18:2 and di-18:3 derivatives of PE and PC obtained from Avanti Lipids (Alabaster, Alabama) were used without further purification. Aqueous dispersions (1:1 wt/wt) were prepared by resuspending weighed amounts of lipid in distilled water. The lipid dispersions were prepared, as far as practical, in a N_2-filled glove box to minimise the chances of lipid oxidation. No significant differences were observed in the course of measurements using different batches of lipid measured on four separate occasions.

2.1. X-ray diffraction

Real-time SAXS/WAXS X-ray diffraction measurements were conducted at station 8.2 of the Daresbury Synchrotron Radiation Source. Detailed descriptions of the measuring system have been published elsewhere [11,17,18].

The lipid samples were mounted in a 1-mm thickness cell fitted with mica windows. Temperature control was achieved by the use of a modified THM 600 thermally-controlled microscope hot stage (Linkam, Tadworth (UK)) connected to a liquid-N_2 pump. Sample temperature was monitored using a thermocouple located in the sample cell. The SAXS pattern was measured above the direct beam using a standard Daresbury quadrant detector located at a distance of 1.25 or 3.2 meters. The WAXS pattern was measured below the direct beam using a commercially available curved INEL detector positioned so that the sample lies at the centre of its radius of curvature.

The data-acquisition system allowed 255 diffraction patterns to be collected consecutively with a 10 μs wait-time between patterns. The exposure time for each pattern, unless otherwise noted, was 5 s. Samples were heated or cooled at a rate of $5°C \cdot min^{-1}$ giving a temperature resolution of better than 0.5°C. The quadrant detector was calibrated using the first nine orders of wet rat-tail collagen (repeat distance 67.0 nm). The INEL detector was calibrated using the peaks arising from hexagonal crystalline ice [19] present in the frozen samples as an internal standard.

2.2. Freeze-fracture electronmicroscopy

Lipid samples were thermally quenched from subambient temperatures using the device illustrated in Fig. 1. The lipid, loaded in a standard Balzer sample holder held in a small pair of forceps, was cooled by a stream of N_2 gas pre-cooled by passage through a cooling coil immersed in liquid N_2. The cooling rate, normally $5–10°C \cdot min^{-1}$, was controlled by the gas flow rate. Sample temperature was monitored by a thermocouple within the cooling chamber directly adjacent to the sample. On reaching the desired quench temperature, the shutter at the base of the cooling chamber was opened, the retaining pin released and the sample holder allowed to fall under gravity plunging the sample into a slurry of liquid and solid N_2. Following thermal quenching, the sample was processed using a Polaron freeze-fracture device. The resulting replicas were examined using a Philips EM301G electron microscope.

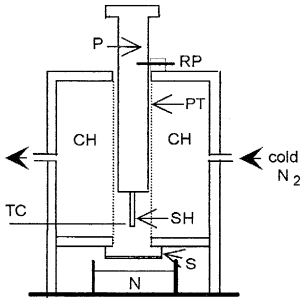

Fig. 1. Schematic diagram of the low-temperature equilibration system used for pre-cooling lipid samples prior to thermal quenching from low temperatures. SH, sample holder; TC, thermocouple; PT, perforated copper tube; CH, cooling chamber containing loosely packed glass-wool; P, heavy metal piston; RP, retaining pin; S, shutter, and N liquid/solid N_2 slurry.

3. Results

3.1. Main phase transitions

Aqueous dispersions of di-18:2 and di-18:3 PE show very similar patterns of phase behaviour at low temperatures. As we have shown elsewhere [11], both lipids are in the H_{II} phase at room temperature, convert to L_α phases on freezing and undergo broad second order transitions spanning about 40°C to form a relatively disordered L_β at temperatures below about $-60°C$.

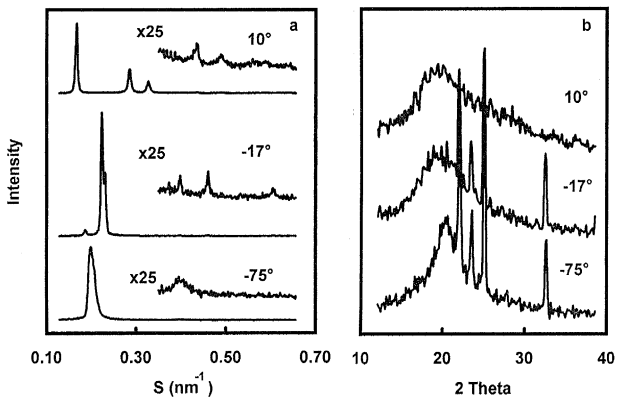

Fig. 2. Typical X-ray diffraction patterns for the H_{II} (top), L_α (middle) and L_β (bottom) phases of aqueous dispersions of di-18:3 PE in (a) the SAXS and (b) the WAXS regions.

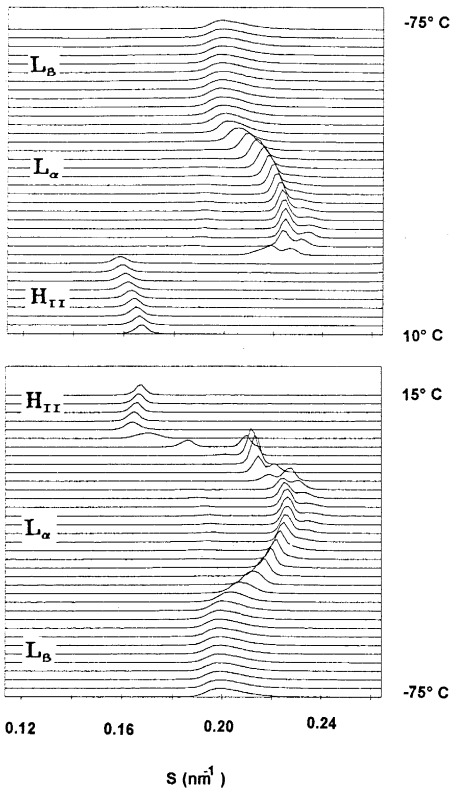

Fig. 3. SAXS diffraction patterns collected for an aqueous dispersion of di-18:3 PE (a) cooled from 10°C to −75°C at a rate of 5°C·min^{-1}. (b) reheated from −75°C to 15°C at the same rate. Patterns correspond to every seventh pattern in series of 255 patterns of 5 s duration.

Typical SAXS/WAXS diffraction patterns for these different phases for di-18:3 PE are presented in Fig. 2. In the case of the H_{II} phase, SAXS diffraction maxima corresponding to the series 1, $1/\sqrt{3}$, $1/\sqrt{4}$, $1/\sqrt{7}$ and $1/\sqrt{9}$ were readily detectable. Only the first two orders of the L_α and L_β phases were detectable but freeze-fracture measurements (see below) confirmed that the samples were predominantly bilayer. While the SAXS diffraction patterns of the H_{II} and L_β phases indicate the existence of single phases, the patterns obtained for the L_α phase, as discussed below, invariably contained additional contributions from other phases.

Distinction between the L_α and L_β phases is based on WAXS measurements. The H_{II} and L_α phase, as illustrated in Fig. 2b, are characterised by a broad maximum centred at about $2\Theta = 20°$ (d = 0.445 nm) and the L_β phase by a rather sharper maximum centred at about $2\Theta = 21.3°$ (d = 0.418 nm). A discussion of the origin of these patterns has been presented elsewhere [11]. The sharp diffraction maxima centred at $2\Theta = 22.8°$, 24.2°, 26.0° and 33.7° in the patterns measured at −17° and −75°C correspond to the 100, 002, 101 and 102 spacings of hexagonal ice [19].

The temperature dependence of these phase changes is illustrated in Fig. 3. The SAXS diffraction patterns shown in Fig. 3a are taken from a series of patterns measured for an aqueous dispersion of di-18:3 PE (50 wt% lipid) cooled at a rate of 5°C.min^{-1}. The

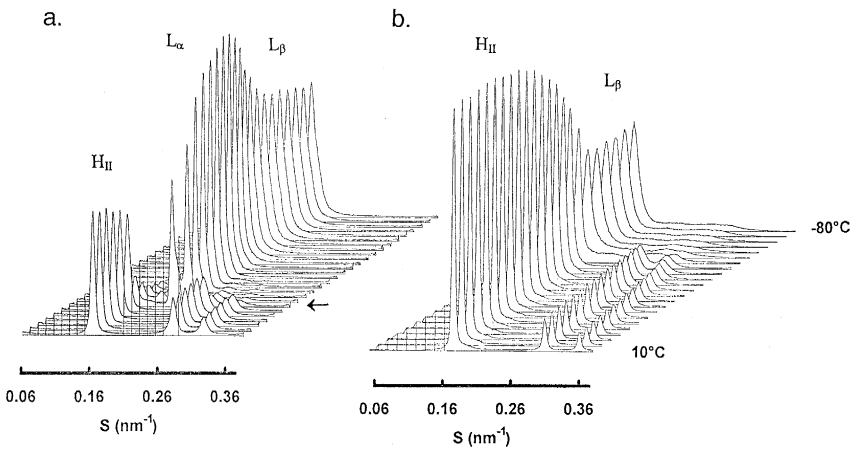

Fig. 4. 3D-representation of the SAXS diffraction patterns collected for a sample of di-18:2 PE dispersed in (a) water and (b) 66 wt% ethylene glycol, cooled from 10°C to −80°C at a rate of 5°C.min^{-1}. The arrow in (a) indicates the onset of freezing in the supercooled aqueous dispersion at about −15°C.

patterns in Fig. 3b were collected on reheating the sample at the same rate. Only the first order diffraction peaks of the H_{II}, L_α and L_β are visible in this representation. The phase sequence on cooling is $H_{II} \rightarrow L_\alpha \rightarrow L_\beta$ and $L_\beta \rightarrow L_\alpha \rightarrow H_{II}$ on heating. Essentially identical results (not shown) were obtained for di-18:2 PE.

The concentrated lipid dispersions used in this study show extensive supercooling. The onset of freezing, however, is easily detected by the emergence of sharp WAXS diffraction maxima associated with crystalline ice of the type shown in Fig. 2b. The sample giving rise to the results shown in Fig. 3a started to freeze at -16°C. On the first sign of ice formation, the repeat spacing of the diffraction pattern of the H_{II} phase rapidly decreased from an initial spacing of $S = 0.161$ nm^{-1} ($d = 6.2$ nm) to a spacing of about $S = 0.234$ nm ($d = 4.27$ nm). At the same time, the intensity of the pattern decreased as it was progressively replaced by the first order diffraction maximum of the L_α phase at $S = 0.225$ nm^{-1} ($d = 4.40$ nm).

This transition, it must be emphasized, is driven by ice formation. In the presence of cryoprotectants to prevent ice formation, as shown in Fig. 4, the lipid remains in the H_{II} phase to temperatures as low as -50°C.

The rapid shrinkage of the repeat spacing of the H_{II} phase is associated with the withdrawal of water from the aqueous channels of the inverted cylindrical micelles making up this phase as water migrates to the advancing ice front. While the bulk of the sample is converted to the L_α phase on freezing, a small fraction of the sample, as illustrated in the freeze-fracture data described below, remains in a non-bilayer configuration. The presence of this non-bilayer lipid is reflected in the peak centred at a slightly shorter spacing about $S = 0.223$ nm^{-1} ($d = 4.29$ nm) than the first order L_α maximum (Fig. 5a) and the emergence of a new low intensity maximum with a rather longer spacing of about $S = 0.195$ nm^{-1} ($d = 5.12$ nm) shown in Fig. 5b.

As the temperature of the sample continues to fall, the repeat spacing of the lamellar phase slowly increases as the lipid undergoes a slow second order $L_\alpha \rightarrow L_\beta$ phase transition spanning about 40°C [11]. Maximum chain extension is seen at about -55°C. Below this temperature, the sample enters the relatively disordered L_β phase reflected in the WAXS diffraction pattern shown in Fig. 2b. The diffraction

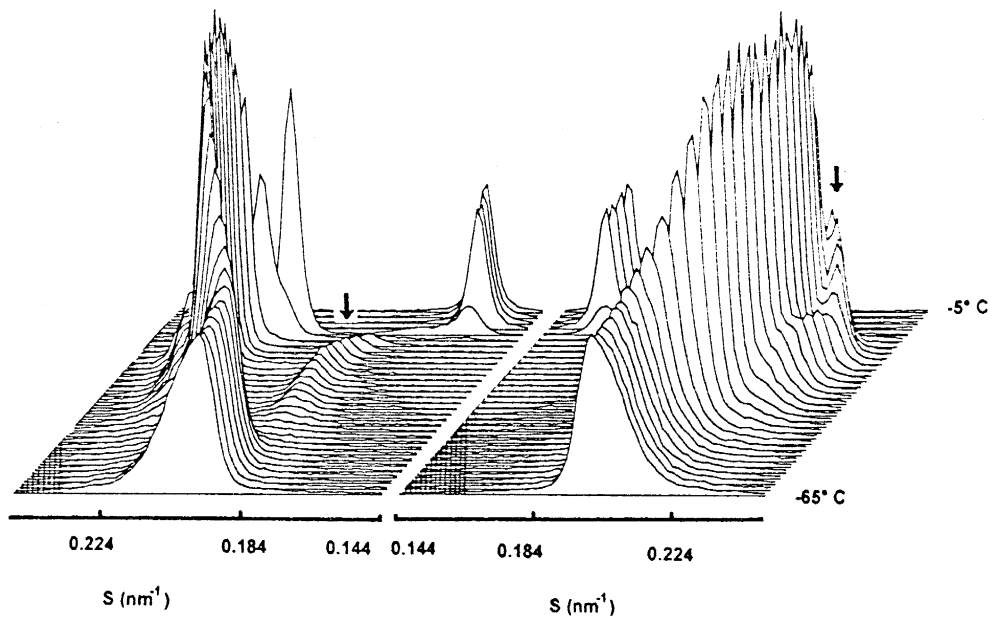

Fig. 5. 3D-representations of the SAXS diffraction patterns shown in Fig. 3 emphasising the appearance of diffraction maxima (arrowed) at (a) narrower and (b) wider spacings than the first order diffraction maximum of the L_α phase seen on conversion of the sample from the H_{II} to the L_α phase.

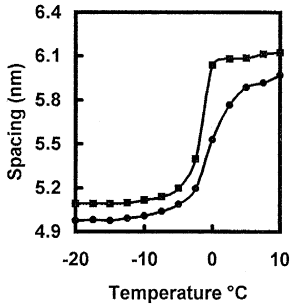

Fig. 6. Temperature dependencies of the d-spacing of frozen aqueous dispersions of di-18:2 (■) and di-18:3 PC (●) heated at a rate of 5°C.min^{-1}.

maxima associated with residual non-bilayer components also disappear at about this temperature.

The changes in diffraction pattern seen on reheating the sample are essentially a reversal of those seen on cooling. The main difference is that the formation, and the expansion, of H_{II} is limited by the amount of unfrozen water in the sample. This is reflected in an initially slow, but rapidly accelerating, increase in the spacing of the first order H_{II} maximum as the temperature of the sample rises above about −20°C. A similar expansion is observed in the d-spacing of equivalent samples of frozen di-18:2 and di-18:3 PC under these conditions (see Fig. 6), underlining the fact that appreciable melting of ice takes place in lipid samples over this temperature range. In the case

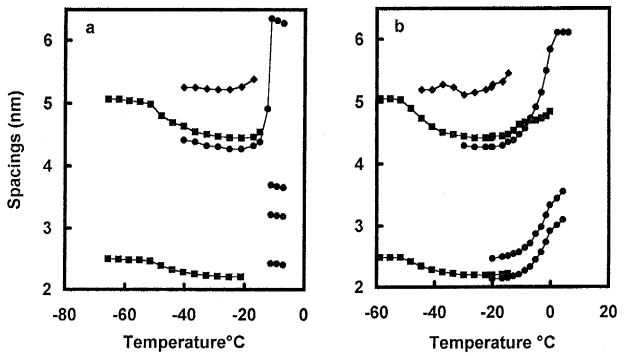

Fig. 7. Temperature dependence of the changes in spacing corresponding to the main SAXS diffraction maxima seen in aqueous di-18:3 PE dispersions (a) cooled from −5° to −75°C at 5°C.min^{-1}, (b) reheated from −60°C to 5°C at the same rate. Spacings relate to the first and second order lamella repeat maxima (■) and the maxima flanking the narrow (●) and the wide angle (♦) sides of the first order lamella repeat maximum (cf., Fig. 5).

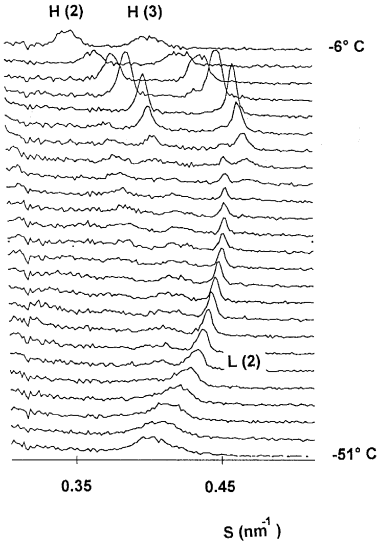

Fig. 8. Series of diffraction patterns showing the changes in the higher order diffraction maxima associated with the formation of the H_{II} phase, occurring as an aqueous dispersion of di-18:3 PE is reheated through the temperature range associated with its $L_\alpha \rightarrow H_{II}$ transition. Note the similarity in spacing of the second order L_α and the $1/\sqrt{4}$ H_{II} maxima L(2) and H(3) respectively.

of heating, it is the L_α phase that persists as a residual component finally disappearing at 0°C as the bulk of the ice melts. A summary of the changes in

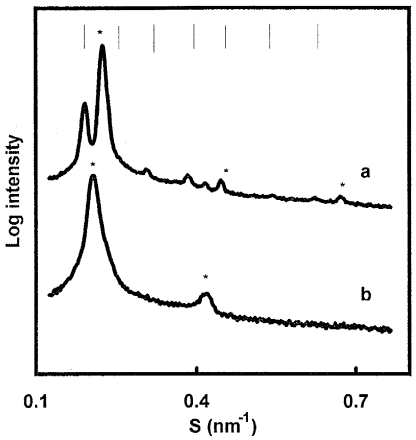

Fig. 9. Logarithmic plot of SAXS diffraction patterns of an aqueous dispersion of di-18:3 PE collected at (a) −21.5°C, (b) −47.5°C. Tick-marks indicate anticipated positions of maxima indexing in the series $1/\sqrt{2}$, $1/\sqrt{3}$, $1/\sqrt{5}$, $1/\sqrt{8}$, $1/\sqrt{9}$, $1/\sqrt{12}$ and $1/\sqrt{21}$ with a unit cell dimension of 7.37 nm. Asterisks mark the first, second and third order maxima of the L_α phase (d = 4.50 nm).

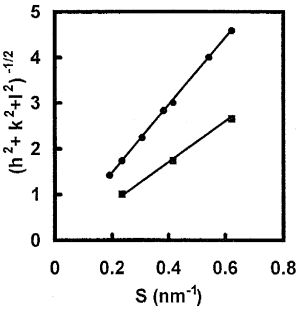

Fig. 10. Plot of the spacings of diffraction maxima for the putative cubic (●) and the H_{II} (■) phases shown in Fig. 9.

spacing of the main diffraction maxima of di-18:3 PE illustrated in Figs. 3 and 5, is presented in Fig. 7. Essentially identical results were obtained for di-18:2 PE. A small increase was observed in the $H_{II} \rightarrow L_{\alpha}$ transition temperature from -20°C to -15°C. The same value of -15°C for the di-18:2 PE has been reported using ^{31}P-NMR [14].

3.2. Residual non-bilayer components

Diffraction patterns showing the changes in the higher order diffraction maxima associated with the formation of the H_{II} phase occurring as the di-18:3 PE sample is reheated through the $L_{\alpha} \rightarrow H_{II}$ phase transition are presented in Fig. 8. They reveal two interesting points. Firstly, they demonstrate the near identity of the spacings of the second order peak of the L_{α} phase and the third order $(1/\sqrt{4})$ peak of the H_{II} phase at the point of first appearance of the H_{II} phase at about -20°C. The d-spacings of the L_{α} and the H_{II} phases (4.41 and 4.27 nm, respectively) are almost identical at the point that the bulk of the

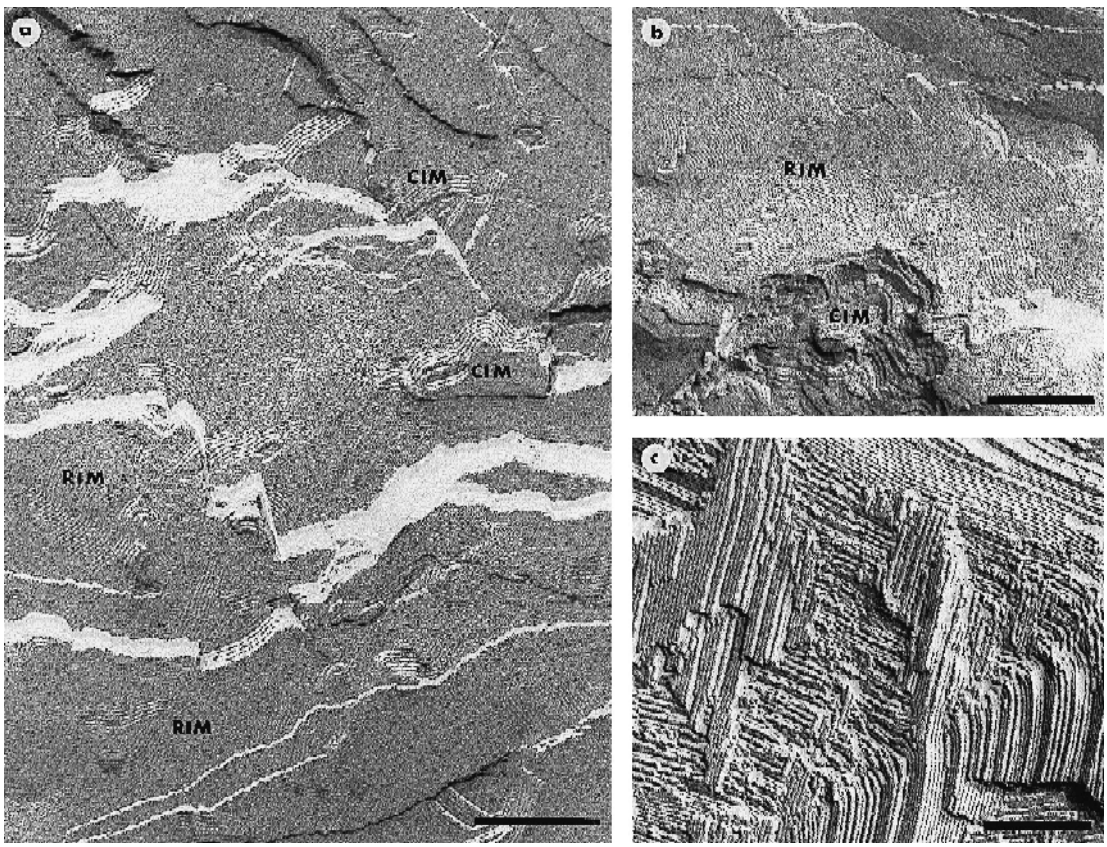

Fig. 11. Freeze-fracture electronmicrographs showing different types of non-bilayer structures commonly observed in aqueous di-18:2 PE dispersions thermally quenched from temperatures below -20°C. (a) and (b) examples of curved whorls of cylindrical inverted micelles (CIM) and residual impressions of such micelles (RIM) (c) overlying layers of CIM. Samples (a) and (c) were thermally quenched from -35°C and (b) from -80°C. Magnification bars are 200 nm.

sample begins to transfer from the L_α to the H_{II} phase.

The second feature of interest is the presence of a number of extremely low intensity higher order diffraction peaks at spacings between that of the first and second order lamellar spacings. These are shown in more detail in the diffraction patterns presented in Fig. 9. The first pattern in this series was collected at −21.5°C and shows the existence of at least two, possibly three, series of peaks. The first series consists of the first, second and third order diffraction peaks of the L_α phase. The second series index in the sequence $1/\sqrt{2}$, $1/\sqrt{3}$, $1/\sqrt{5}$, $1/\sqrt{8}$, $1/\sqrt{9}$, $1/\sqrt{16}$ and $1/\sqrt{21}$ with a unit cell of 7.4 nm. The $1/\sqrt{3}$ maximum is difficult to resolve from the first order lamellar spacing using the camera length employed in this measurement but is clearly visible in measurements using longer camera lengths (cf. Fig. 5a). The $1/\sqrt{3}$, $1/\sqrt{9}$ and $1/\sqrt{21}$ maxima in this series, as illustrated in Fig. 10, are coincident with the 1, $1/\sqrt{3}$, $1/\sqrt{7}$ maxima of an H_{II} phase with a d-spacing of 4.27 nm. No $1/\sqrt{12}$ maximum (corresponding to a $1/\sqrt{4}$ H_{II} maximum) is observed at this temperature although such a peak is clearly observable at temperatures above that of the L_α-H_{II} phase transition (cf. Fig. 8).

We provisionally assign this second series of peaks to an as yet unidentified cubic phase but recognize that the $1/\sqrt{3}$, $1/\sqrt{9}$ and $1/\sqrt{21}$ peaks might also contain contributions from the 1, $1/\sqrt{3}$ and $1/\sqrt{7}$ peaks of H_{II} phase lipid. The second diffraction pattern shown in Fig. 9 was collected at −47.5°C and only the first and second order maxima of the L_α phase are visible. The putative cubic phase appears to disappear at temperatures below about −35°C. It reappears on heating, however, even after storage of the samples for 30 min at −80°C.

3.3. Freeze-fracture electronmicroscopy

Replicas prepared from dispersions of di-18:2 PE equilibrated and thermally quenched from tempera-

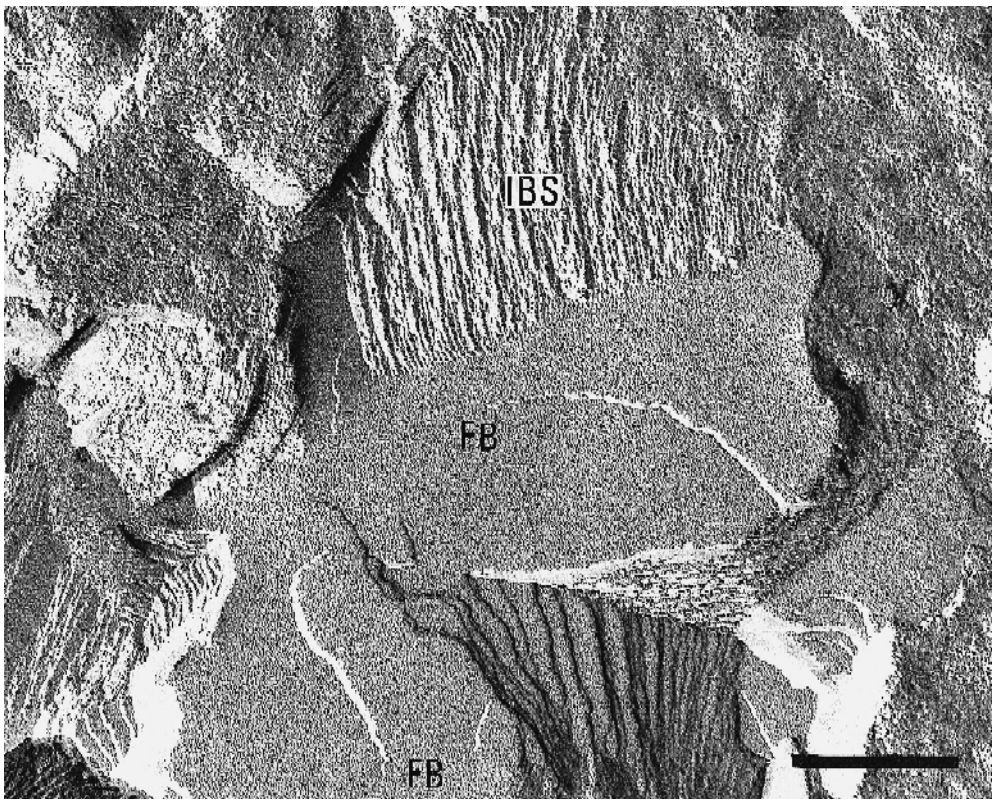

Fig. 12. Freeze-fracture electronmicrograph of aqueous di-18:2 PE dispersions thermally quenched from −35°C showing intersecting bilayer stacks (IBS). Note also examples of the fusion of overlying bilayers (FB). Magnification bar 200 nm.

tures above 0°C confirmed that the unfrozen lipid was in the H_{II} phase (results not shown). Samples thermally quenched from below −20°C were predominantly bilayer but contained significant amounts of non-bilayer structure. This non-bilayer material manifested itself in a wide variety of different structures. The most common features were small inclusions of cylindrical inverted lipid micelles, and ripple-like structures that appear to be residual impressions of such micelles, of the type shown in Fig. 11a,b. The amount of non-bilayer material decreased with the thermal quenching temperature but there was clear evidence for the presence of such material even in samples quenched from −80°C.

Although structures in which different layers of cylindrical micelles cross each other at right angles were occasionally observed (Fig. 11c), we were unable to find any structures in our samples that we could unequivocally identify as cubic phase lipid. Our diffraction measurements suggest that if cubic phase lipid is formed in our samples, it is likely to be present only at a very limited temperature range (−20° to −35°C). There is thus a strong possibility that our thermal quenching rates were insufficiently rapid to preserve such structures.

A particularly interesting feature of our replicas was the presence of intersecting bilayer stacks of the type shown in Fig. 12. The presence of such structures is consistent with the epitaxial growth of stacked bilayers along the equivalent intersecting (1,1), (0,1), (1,0) planes of the H_{II} lattice. A diagrammatic representation of the possible molecular organisation of the lipids in such structures is provided in Fig. 13a. Another common feature of our replicas, also visible in the electronmicrograph presented in Fig. 12, is the fusion of two parallel bilayer sheets. A possible molecular organisation for these features is shown in Fig. 13b.

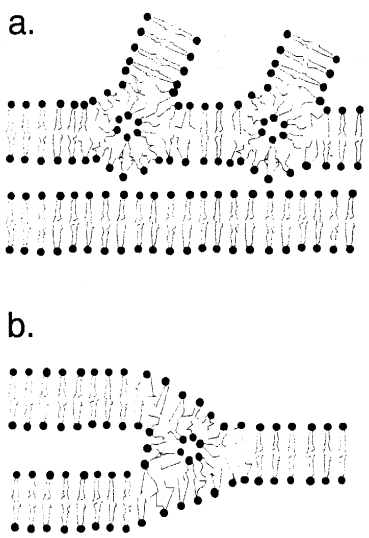

Fig. 13. Diagrammatic representation of the possible molecular organisation of (a) the intersecting bilayer stacks and (b) the fused bilayer regions shown in Fig. 12.

4. Discussion

The measurements described in this paper relate to the low temperature bilayer to non-bilayer transitions taking place in aqueous dispersions of the di-18:2 and di-18:3 derivatives of PE. In the absence of ice, these lipids persist in the H_{II} phase to temperatures at least as low as −50°C (Fig. 4). The fact that aqueous dispersions of the lipids undergo a rapid transition from the H_{II} to the L_{α} phase on freezing (Fig. 7a) and that their return to the H_{II} phase on reheating coincides with the onset of swelling of their lamellar phase (Fig. 7b) indicates that the H_{II}-L_{α} transition in these lipids is controlled by the availability of unfrozen water.

4.1. L_{α}-H_{II} transition in frozen samples

The driving forces behind the formation of the H_{II} phase under normal conditions are well understood (see the review of Seddon [20] and the Refs. therein). With increasing temperature, the imbalance between the lateral pressure of repulsion exerted by the hydrocarbon chains of the lipid bilayer, as a consequence of their kinetic energy, and tension in the headgroup region arising from hydrophobic, steric, hydrational and electrostatic effects serve to place the opposed monolayers of the lipid bilayer into a state of increasing *frustration*. This is relieved by a decoupling of the monolayers to form cylindrical inverted micelles with negative surface curvatures. The diameter and packing of these micelles is determined by the necessity of filling the hydrocarbon interior of the phase with the lipid chains [21,22].

The radius of curvature of the inverted micelles making up the H_{II} phase varies with temperature;

decreasing with increased temperature, as the kinetic energy of the chains increases, and increasing with decreased temperature, as their kinetic energy falls. Conversion back to the L_α phase is normally triggered when the radius of curvature of the cylindrical micelles becomes so large that a continuous hydrophobic phase cannot be maintained between the micelles.

The sequence of events occurring on freezing aqueous dispersions of H_{II} phase lipid is very different. Ice formation reduces the amount of water available to fill the cylindrical tubes of the H_{II} phase. This leads to a rapid decrease in tube diameter and hence d-spacing (Fig. 3a and Fig. 7a). The shrinking tubes can lengthen in order to maintain the surface area available to the lipid headgroups. Their increased surface curvature, however, causes an imbalance between the forces acting in the surface layer and the hydrophobic core of the lipid phase. A point will be reached where this imbalance prevents any further reduction in tube radius and the lipid reverts to a bilayer configuration. Further reductions in aqueous volume can then be accommodated by shrinkage of the unfrozen inter-bilayer aqueous layer with no net reduction in surface area and the natural tendency of the lipid chains to straighten with lowered temperature can occur.

Tate et al. [23] estimated a limiting value for the tube radius r_t of the emerging H_{II} phase of dioleoyl phosphatidyl-ethanolamine on the assumption that the local water concentration ϕ_w remains constant throughout the transition. Their method of calculation is not suitable for frozen dispersions as it requires a knowledge of the values of the partial volume contributions of lipid and water. However, using the same basic assumption of constant water content, a good approximation can be made on purely geometric grounds.

The volume of interlamellar water corresponding to a single tube of H_{II} lipid at the point of phase conversion, V, as can be appreciated by reference to Fig. 14a, is given by:

$$V = d_w \times 2d_H/\sqrt{3} \times l_t = \pi r_t^2 \times l_t \quad (1)$$

where d_w is the thickness of the interlamellar water layer, d_H is the repeat distance of the H_{II} phase, l_t the length and r_t the radius of the cylindrical micelles. Substituting $(d_L\text{-}2d_l)$ for d_w, where d_L equals

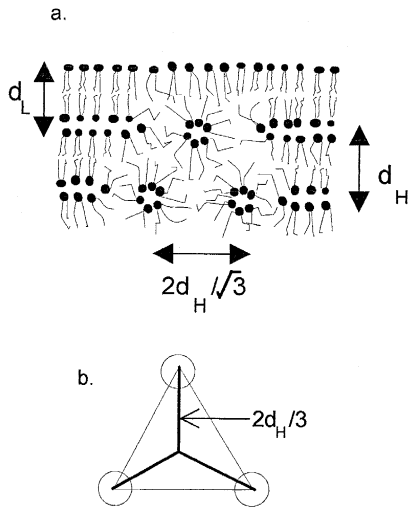

Fig. 14. Diagrams illustrating the spatial relationships between the L_α and emerging H_{II} phases of di-polyenoic PE derivatives at the point of phase transition. See text for details.

the lamellar repeat spacing and $2d_l$ the bilayer thickness:

$$\pi r_t^2 = 2d_H/\sqrt{3}.(d_L - 2d_l) \quad (2)$$

A major constraint on the system, as pointed out by Gruner and his co-workers [21,22], is that the lipid chains must reach the furthest interstitial point of the hydrophobic region. If, as a first approximation, we take the maximum extension of the chains, d_{max}, to be half that of the corresponding bilayer thickness then, as illustrated in Fig. 14b:

$$d_{max} = d_l = 2d_H/3 - r_t \quad (3)$$

Substituting for d_l in Eq. (2) and solving the resulting quadratic using the measured values of 4.41 and 4.27 nm at the point of phase transition for d_L and d_H yields values of 3.89, 0.90, and 0.52 nm for $2d_l$, r_t and d_w respectively. The corresponding equilibrium value for r_t for the supercooled system at -15°C, assuming the same d_{max} value, is 2.29 nm.

This compares with values of 1.62 nm and 2.16 nm calculated by Tate et al. [23] for r_t for di-18:1 PE at its transition point and under equilibrium conditions at 20°C. The smaller value of r_t in the frozen system reflects the very limited amount of unfrozen water available. Direct measurement of the thickness of the unfrozen water layer in our samples is impractical as we observe too few orders of diffraction to calculate accurate electron density profiles. It is, however, noteworthy that our predicted value of 0.52

nm is in fairly good agreement with the value of 0.4 nm calculated by Gleeson et al. [24] for frozen dispersions of di-18:1 PC in this temperature range.

4.2. Possible involvement of a cubic phase

Seddon et al. [20] have demonstrated the existence, at different levels of hydration, of three different types of cubic phase (Pn3m, Im3m and Ia3d) close to the phase boundary between the L_α and H_{II} phases formed by di-12:0 PE. Gruner and his co-workers [25] have demonstrated the formation in dispersions of N-methylated di-18:2 PE of two cubic phases; one that appears to index as a Pn3m or Pn3 phase and the other as an Im3m phase. They have also demonstrated that repeated rapid cycling between -5 and -15°C induces the formation a Pn3m cubic phase in di-18:1 PE dispersions [26].

Our observations suggest the existence in the di-18:2 and di-18:3 PE of an unidentified cubic phase (Q_x) indexing in the ratio $1/\sqrt{2}:1/\sqrt{3}:1/\sqrt{5}:1/\sqrt{8}:1/\sqrt{9}:1/\sqrt{16}:1/\sqrt{21}$, with the $1/\sqrt{3}$, $1/\sqrt{9}$, and $1/\sqrt{21}$ maxima coincident with the 1, $1/\sqrt{3}$ and $1/\sqrt{7}$ maxima of the H_{II} phase. The existence of a $1/\sqrt{5}$ maximum would appear to rule out the existence of Pn3m, Im3m or Ia3d phases, none of which show such a maximum [27]. However, in view of the low intensity of the observed diffraction maxima, any definitive identification of their origin must await the availability of more detailed diffraction patterns. Attempts to increase the fraction of the sample that forms into the cubic phase by repetitive cycling through the transition region along the lines described by Shyamsunder et al. [26] for di-18:1 PE have so far proved unsuccessful.

Formation of cubic phases in single lipid systems of the type studied here does not imply that they are necessary intermediates in H_{II}-L_α transitions. As discussed by Shyamsunder et al. [26], their formation probably reflect the existence of *local* rather than *system* free energy minima in the system. The cubic phase in systems of this type represent metastable states which are readily eliminated when the lipid is cooled to form the L_β phase. However, the di-polyenoic PE derivatives, as we have shown elsewhere [11], have very disordered gel phases. This is reflected in our freeze-fracture measurements that indicate that our samples contain significant amounts of non-bilayer structures even at -80°C. These appear to act as nuclei for regrowth of the cubic phase on reheating.

4.3. Epitaxial relationships

Epitaxial relationships of lamellar and hexagonal phases involving cubic intermediates have been reported for the lyotropic liquid-crystal phases of surfactants [28,29]. There are also reports of an alignment between the d(001) spacing of the L_α phase and the d(222) spacing of a body-centred cubic phase of hydrated 1-monostearin [30] and of an alignment between H_{II} phase and the cubic (222) spacing of an unsaturated acylglycerol system [31]. The present study suggests the existence of the following relationship, associated with epitaxial relationships in frozen aqueous dispersions of di-18:2 and di-18:3 PE:

$$d_{(10)}H_{II} = d_{(111)}Q_x \approx d_{(001)}L_\alpha$$

The similarity in spacings of the H_{II} and L_α phases means that there is minimal displacement of the aqueous phase within the system during the course of the $H_{II} \rightarrow L_\alpha$ transition resulting in the ready formation of intersecting bilayer stacks of the type depicted in Fig. 12. In more hydrated systems, the bulk movement through the samples tends to eliminate such structures. It is probably the same lack of bulk movement of aqueous phase that favours the existence of local free-energy minima associated with the formation of the cubic phase. A clearer picture of the processes involved will, however, have to await a definite identification of the structural organisation of this phase.

Acknowledgements

The valuable assistance and advice of Drs. W. Bras and B.U. Komanschek of Daresbury Laboratory in these measurements are gratefully acknowledged.

References

[1] Coolbear, K.P., Berde, C.B. and Keough, K.M.W. (1983) Biochemistry 22, 1466–1473.
[2] Keough, K.M.W., Giffin, B. and Kariel, N. (1987) Biochim. Biophys. Acta 902, 1–10.

[3] Niebylski, C.D. and Salem, N. (1994) Biophys J. 67, 2387–2393.
[4] Barry, J.A., Trouard, T.P., Salmon, A. and Brown, M.F. (1991) Biochemistry 30, 8386–8394.
[5] Holte, L.L., Peter, S.A., Sinnwell, T.M. and Gawrisch, K. (1995) Biophys. J. 68, 2396–2403.
[6] Litman, B.J., Lewis, E.N. and Levin, I.W. (1991) Biochemistry 30, 313–319.
[7] Keough, K.M.W. and Kariel, N. (1987) Biochim. Biophys. Acta 902, 11–18.
[8] Barton, P.G. and Gunstone, F.D. (1975) J. Biol. Chem. 250, 4470–4476.
[9] Cevc, G. (1991) Biochemistry 30, 7186–7193.
[10] Williams, W.P., Sanderson P.W, Cunningham, B.A., Wolfe D.H. and Lis, L.J. (1993) Biochim. Biophys. Acta 1148, 285–290.
[11] Williams, W.P., Cunningham, B.A., Wolfe D.H., Bras, W., Derbyshire, G.E. and Mant, G.R., (1996) Biochim. Biophys. Acta 1284, 86–96.
[12] Sanderson, P.W. and Williams, W.P. (1992) Biochim. Biophys. Acta 1107, 77–85.
[13] Seddon, J.M., Cevc, G. and Marsh, D. (1983) Biochemistry 22, 1280–1289.
[14] Tilcock, C.P.S. and Cullis, P. (1982) Biochim. Biophys. Acta 684, 212–218.
[15] Epand, R.M. (1985) Chem. Phys. Lipids 36, 387–393.
[16] Sanderson, P.W, Williams, W.P., Cunningham, B.A., Wolfe, D.H. and Lis, L.J. (1993) Biochim. Biophys. Acta 1148, 278–284.
[17] Bras, W., Derbyshire, G.E., Ryan, A.J., Mant, G.R., Manning, P., Cameron, R.E., Mormann, W. (1993) J. Physique IV 3, 447–450.
[18] Cunningham, B., Quinn, P.J., Lis. L.J. and Bras, W. (1994) J. Biochem. Biophys. Methods 29, 87–111.
[19] Dowell, L.G., Moline, S.W. and Rinfret, A.P. (1962) Biochim. Biophys. Acta 59, 229–242.
[20] Seddon, J.M. (1990) Biochim. Biophys. Acta 1031, 1–69.
[21] Gruner, S.M. (1985) Proc. Natl. Acad. Sci. USA 82, 3665–3669.
[22] Tate, M.W. and Gruner, S.M. (1987) Biochemistry 26, 231–236.
[23] Tate, M.W., Shyamsunder, E., Gruner, S.M. and D'Amico, K.L. (1992) Biochemistry 31, 1081–1092.
[24] Gleeson, J.T., Erramilli, S. and Gruner, S.M. (1994) Biophys. J. 67, 708–712.
[25] Gruner, S.M., Tate, M.W., Kirk, G.L., So, P.T.C., Turner, D.C., Keane, D.T., Tilcock, C.P.S. and Cullis, P.R. (1988) Biochemistry 27, 2853–2866.
[26] Shyamsunder, E., Gruner, S. M., Tate, M.W., Turner, D.C., So, P.T.C. and Tilcock, C.P.S. (1988) Biochemistry 27, 2332–2336.
[27] Lindblom, G. (1989) Biochim. Biophys. Acta 988, 221–256.
[28] Kekicheff, P. and Cabane, B. (1988) Acta Cryst. B44, 395–406.
[29] Rançon, Y. and Charvolin, J. (1988) J. Phys. Chem. 92, 2646–2651.
[30] Lindblom, G., Larsson, K., Johannson, L., Fontell, K. and Forsen, S. (1979) J. Am. Chem. Soc. 101, 5465–5470.
[31] Larsson, K., Fontell, K. and Krog. N. (1980) Chem. Phys. Lipids 27, 321–328.